J Sol-Gel Sci Technol (2009) 49:355–363
DOI 10.1007/s10971-008-1866-1

ORIGINAL PAPER

Luminescence and oxygen sensing properties of ORMOSILs covalently grafted with a novel ruthenium(II) complex

Xiudong Wu · Yan Cong · Yanhong Liu · Jun Ying · Bin Li

Received: 24 September 2008 / Accepted: 20 November 2008 / Published online: 4 December 2008

Abstract A series of VTES/TEOS composite xerogels covalently grafted with a novel complex $Ru(phen)_2(Dppz\text{-}Si)Cl_2$ were prepared, using the alkoxysilane-modified dipyrido[3,2-a:2′,3′-c]phenazine compound (denoted as Dppz-Si) as the second ligand of the $Ru(phen)_2Cl_2$ (phen = 1,10-phenanthroline) complex and a precursor of the sol–gel process. Bulk xerogels were obtained by co-hydrolyzing and co-condensation from a mixture of triethoxysilane (TEOS), $Ru(phen)_2(Dppz\text{-}Si)Cl_2$ and Vinyltriethoxysilane (VTES). The luminescence intensity of composite xerogels is enhanced by 18.2 times, and the sensitivity is improved from 1.1 to 3.1 by optimizing the molar ratio of VTES to TEOS. The composite xerogel containing 80% VTES in precursor was optimal, exhibiting the maximum luminescence intensity and sensitivity. These results indicate that the complex $Ru(phen)_2(Dppz\text{-}Si)Cl_2$ is sensitive to oxygen concentration, VTES is a kind of excellent organic modifier and can greatly improved photoluminescent (PL) and oxygen sensing performances.

Keywords Oxygen sensor · ORMOSILs · Covalent grafting · Ruthenium(II) complex

X. Wu · J. Ying
Department of Chemistry, Polyoxometalate Science Key Laboratory of Ministry of Education, Northeast Normal University, Changchun 130024, People's Republic of China

Y. Cong · Y. Liu · B. Li (✉)
Key Laboratory of Excited State Processes, Changchun Institute of Optics Fine Mechanics and Physics, Chinese Academy of Sciences, Changchun 130033, People's Republic of China
e-mail: lib020@yahoo.cn

1 Introduction

Determination of oxygen concentration is quite critical for the very existence of life. Recent interest in the methods for measuring oxygen concentration has been focused mainly on optical sensors due to their advantages over conventional amperometric electrodes in that they are faster, do not consume oxygen, and are not easily poisoned [1–4]. For the sensing dyes, Ruthenium(II) complexes have been frequently utilized owing to their high photochemical stability, high extinction coefficient, relatively long lifetime determined by the metal to ligand charge transfer (MLCT) excited state, large Stokes shift, and absorption spectrum of inexpensive, commercially available blue LED's [5–9].

As for the host materials, sol–gel synthesis is a versatile technique in which the physical, chemical, and optical properties of the silicate based gels are easily tailored [10, 11]. With the development of the sol–gel science and technology, the preparation of organically modified silicates (ORMOSILs) becomes one of the attractive features of the sol–gel process. The ORMOSILs provide significant changes in the quenching behavior of the guest Ru(II) molecules, because the non-hydrolyzing alkyl groups structurally acting as a network modifier that terminates the silicate networks [12, 13]. A typical process of preparing such ORMOSILs is by co-hydrolyzing from a mixture of a tetraalkoxysilane and an alkyl-substituted silicon alkoxides.

However, many studies were mainly focused on the sol–gel martrix doped with the Ru(II) complexes in which only weak physical interactions exist between the Ru(II) complexes and the martrix. As a result there are significant drawbacks when these systems are used as oxygen sensors, including inhomogeneous distribution and leaching of dopants [12, 14, 15]. Recently, oxygen sensors covalently

bonded with Ru(II) complexes have shown enhanced stability of oxygen sensor properties and anti-leaching of dopants [16, 17], but luminescence and oxygen sensing properties of ormosils covalently grafting Ru(II) complex are still expected to be further studied.

In this paper, we describe the fabrication of a series of materials covalently bonded with a novel Ru(II) complex $Ru(phen)_2(Dppz\text{-}Si)Cl_2$ (depicted in Scheme 1) by sol–gel process using ORMOSILs as matrix, in which VTES was selected as an organic modifier in the precursor. It is interesting that the luminescence and oxygen sensing properties of these composite xerogels showed a strong dependence on the molar ratio of VTES to TEOS. The luminescence intensity is enhanced by 18.2 times, and the sensitivity is enhanced from 1.1 to 3.1 by optimizing the molar ratio of organic modifier VTES to TEOS. To the best of our knowledge, this is the first time to report PL and oxygen sensing properties of organically modified oxygen sensing materials covalently bonded with Ru(II) complex in the open literature.

2 Experimental

2.1 Chemical regents

The anhydrous $RuCl_3$ (99.99%), VTES, 3,4-Diamino-benzoic acid, along with the 3-aminopropyltriethoxysilane (APS) were obtained from Aldrich (Milwaukee, WI. USA) and were used without further purification. The TEOS and ethanol (EtOH) were purchased from Tianjin Chemicals Company. The concentrated HCl and thionyl chloride ($SOCl_2$, A.R.) were obtained from Shanghai Chemical Company. $SOCl_2$ was used after distillation in vacuo. The complex bis(1,10-phenanthroline)ruthenium(II) chloride dihydrate, $Ru(phen)_2Cl_2 \cdot 2H_2O$ was synthesized and purified as described in the literature [18]. 1,10-phenanthroline-5,6-dione was prepared according to the literature [19]. The water used in our present work is de-ionized.

2.2 Sample preparation

2.2.1 *Synthesis of hydrolysable functionalized Dppz-Si ligand*

The ligand Dppz-Si was synthesized using dipyridophenazine-11-carboxylic acid (denoted as Dppa) and APS as the starting materials similar to the previous publication with some minor modifications [20, 21]. Dppa was conveniently synthesized by the condensation of 1,10-phenanthroline-5,6-dione and 3,4-diamino-benzoic acid according to the literature [22]. The detailed synthetic procedure can be briefed as follows: Dppa (0.326 g; 1 mmol) was dissolved in excess distilled $SOCl_2$ (8 mL) and refluxed for 4 h, the excess $SOCl_2$ was eliminated by evaporation from the ferrugineous solution, and the residual was reacted with APS under nitrogen for 4 h at room temperature and using chloroform as a solvent (40 mL). The solution was filtered and evaporation of the residual organic solvent gave the alkoxysilane-modified dipyrido[3,2-a:2′,3′-c]phenazine ligand Dppz-Si.

2.2.2 *Synthesis of the hydrolysable Ru (phen)$_2$ (Dppz-Si)Cl$_2$*

A mixture of $Ru(phen)_2Cl_2$ and Dppz-Si in anhydrous ethanol was refluxed for 8 h in nitrogen atmosphere to give a transparent deep red solution, indicating that the complexation reaction between Dppz-Si and $Ru(phen)_2Cl_2$ had finished. The molar ratio of Dppz-Si to $Ru(phen)_2Cl_2$ was 1.02:1. Further purification of the complex was obtained by slow vapor diffusion of diethylether into ethanol solution of the obtained Ru $(phen)_2(Dppz\text{-}Si)Cl_2$.

2.2.3 *Preparation of Ru-doped xerogels*

A pure TEOS-derived xerogel was prepared by resolving $Ru(phen)_2(Dppz\text{-}Si)Cl_2$ (12.72 mg) in ethanol (5.2 mL) in a plastic vial and stirred for 5 min, and then 5 mL of TEOS was added for another 5 min stirring, by subsequently H_2O and HCl addition. The final mole ratio of constituents was $TEOS{:}H_2O{:}C_2H_5OH{:}HCl = 1{:}4{:}4{:}0.01$. The concentration of $Ru(phen)_2(Dppz\text{-}Si)Cl_2$ in the final sol was 2×10^{-3} M. The solution was kept stirring at room temperature for 4 h. The xerogel were dried at 60 °C in vacuo for 24 h, and then optical transparent crack-free monolithic xerogel was obtained. Finally, the transparent monolithic xerogel was powdered for characterization (denoted as sample *a*). This procedure was chosen because it is representative of xerogels reported in the literatures [15, 23–25].

The synthetic procedure of VTES/TEOS composite xerogels was similar to the above preparation of TEOS-based xerogel with some minor modifications by mixing TEOS and VTES together to form solutions that contained 20, 40, 60, 80, 100 mol% VTES (denoted as sample *b*, *c*, *d*, *e*, and *f* individually).

2.3 Instruments and measurements

The infrared absorption spectra were measured in the region of 400–4,000 cm^{-1} by a Fourier transform infrared (FT-IR) spectrophotometer (Model Perkin-Elmer Model 580B) with a resolution of ± 4 cm^{-1} using the KBr pellet technique.

The oxygen sensing properties of the obtained samples were investigated based on the luminescence intensity

Scheme 1 Synthetic procedure of xerogels containing Ru(II) complex and their predicted structure

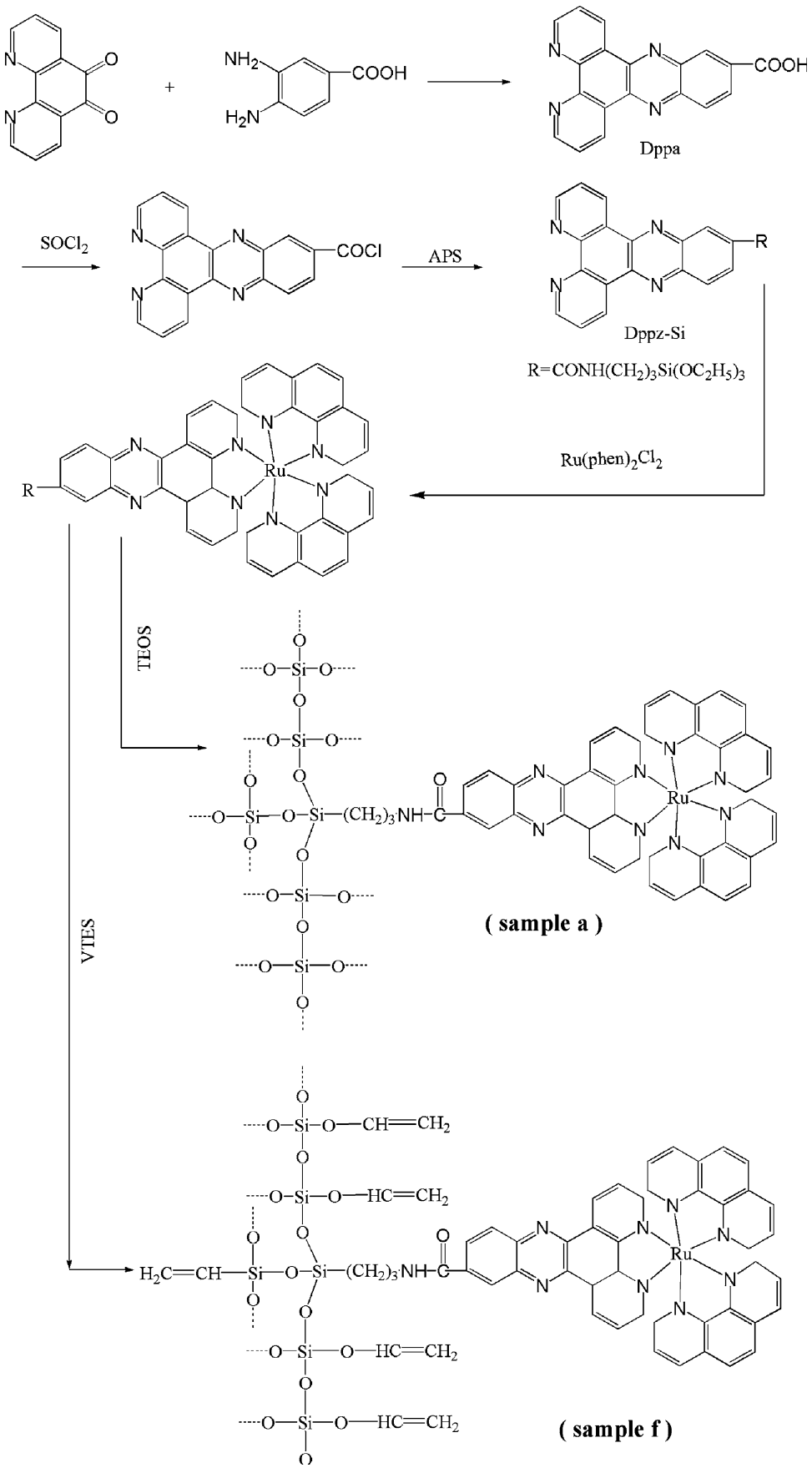

quenching instead of the excited-state lifetime because it is hard to obtain the precise excited state lifetime values under quenched conditions. Luminescence intensities were characterized using a Hitachi-4500 fluorescence spectrophotometer equipped with a xenon lamp (150 W) operating in the 200–900 nm range. The excitation wavelength was 480 nm. The excitation spectra were obtained monitoring at the wavelength of peak emission (590 nm).

For the Stern–Volmer plot measurement, oxygen and nitrogen were mixed at different concentrations via gas-flow controllers and flowed directly into the gas chamber sealed with a close fitting suba-seal rubber lid equipped with two (IN and OUT) tubes [17]. We typically allowed 1 min between changes in the N_2/O_2 concentrations to ensure that a new equilibrium point had been established. Equilibrium was evident when the luminescence intensity remained constant (±2%).

In the fluorescence lifetime measurement of the *Ru-doped xerogels* covalently bonded with Ru(Π) complex, a 266 nm light generated from the Fourth-Harmonic-Generator pumped by the pulsed Nd:YAG laser was used as excitation source. The Nd:YAG laser was with a line width of 1.0 cm^{-1}, pulse duration of 10 ns and repetition frequency of 10 Hz. A Rhodamine 6G dye pumped by the same Nd:YAG laser was used as the frequency-selective excitation source. All measurements were performed at room temperature.

3 Results and discussion

3.1 Structural analysis

The complex $[Ru(phen)_2Dppz]Cl_2$ has been covalently grafted to the silica-based networks for oxygen sensors by using the double-role Dppz-Si compound, as a second ligand for $Ru(Bphen)_2Cl_2$ and a precursor of the ORMOSILs. The synthesis procedure is outlined in Scheme 1.

Since VTES has three ethoxy-groups that undergo hydrolysis (whereas TEOS has four), only three linkages may form bridging oxygen bonds that contribute in the development of the silicate network. The vinyl species show a poor affinity for water and do not undergo hydrolysis acting as network terminator throughout the sol–gel process. The surface Si–OH groups are mostly replaced by the $Si–CH=CH_2$. And the number of surface $Si–CH=CH_2$ groups increases as increasing the molar ratio of VTES, which is further evidenced by FT-IR. Hence, the silicate network has terminating groups in the form of the organic $Si–CH=CH_2$ species and yield a more open structure, a less rigid as well as a more hydrophobic condition than the TEOS-based xerogel [26–28].

3.2 FT-IR spectra results

The successfully covalent-grafting of Ru $(phen)_2(Dppz\text{-}Si)Cl_2$ to silicates can be supported by the FT-IR spectra of each product. Patterns a–g of Fig. 1 show the FT-IR spectra of, TEOS-based xerogel (*a*), VTES/TEOS composite xerogels (*b*, *c*, *d*, *e*, and *f*) and hydrolysable $Ru(Phen)_2(Dppz\text{-}Si)Cl_2$ complex (*g*) respectively. In Fig. 1g, the spectrum of $Ru(Phen)_2(Dppz\text{-}Si)Cl_2$ is dominated by *v*(Si–C, 1,204 cm^{-1}) and *v*(Si–O, 1,090 cm^{-1}) adsorption bands, which are the characteristics of trialkoxylsilyl functions [29]. The adsorption bands at 1,650 and 1,627 cm^{-1} due to the adsorption of amide groups (CONH) indicate that APS has been successfully grafted on to dipyrido[3,2-*a*:2′,3′-*c*]phenazine (Dppz) [20, 21]. Further evidence for this is the presence of the bending vibration of Si–O at 465 cm^{-1} (from APS) [20, 21]. In Fig. 1a–f, the adsorption bands near 1,084 cm^{-1} (ν_{as}, Si–O), 799 cm^{-1} (ν_s, Si–O), and 461 cm^{-1} (δ, Si–O–Si) (*v* represents stretching, δ in-plane bending, s symmetric, and as asymmetric vibrations) substantiate the formation of the silica framework [20]. The

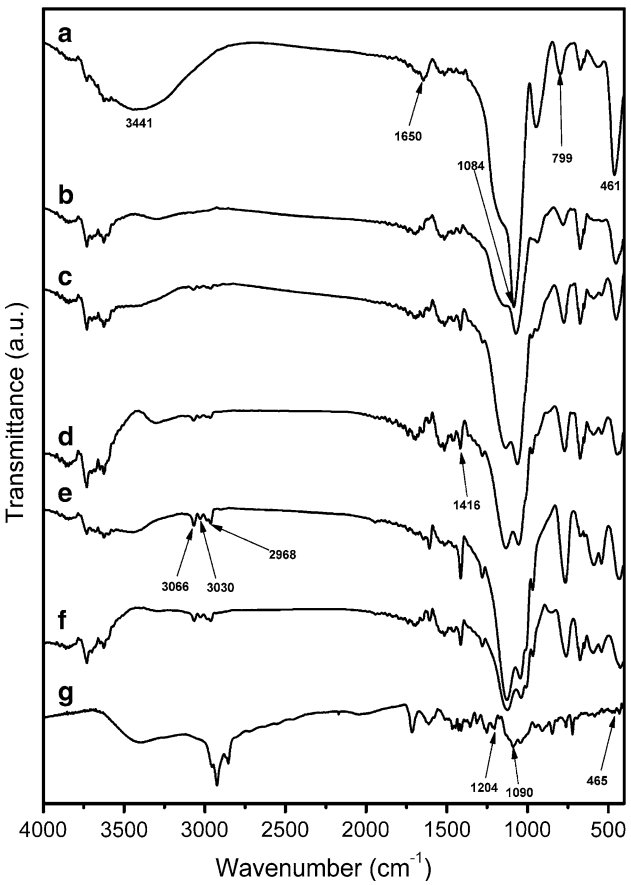

Fig. 1 FT-IR spectra for Ru-doped xerogels. **a** 100% TEOS; **b** 80% TEOS/20% VTES; **c** 60% TEOS/40% VTES; **d** 40% TEOS/60% VTES; **e** 20% TEOS/80% VTES; **f** 100% VTES; **g** hydrolysable $Ru(Phen)_2(Dppz\text{-}Si)Cl_2$ complex

peaks at 1,650 cm^{-1}, originating from the CONH group of Dppz-Si, can also be observed in the final materials, which is consistent with the fact that the Dppz-Si group in the framework remains intact after hydrolysis/condensation reaction. The ν(Si–C) vibration located at 1,204 cm^{-1} is still observed in the IR spectrum of the final materials, indicating that there is not a great extent of Si–CH_2 bond cleavage occurring [20].

In addition, sharp vibration peaks near 3,030 cm^{-1} (originating from Si–CH=CH_2) and adsorption at 1,416 cm^{-1} (–CH=CH_2) appear in Fig. 1b–f, which are not found in Fig. 1a, suggesting the presence of vinyl in the ORMOSILs. Furthermore, compared with Fig. 1 a–f, the intensity ratio of the adsorption peaks located near 3,030 cm^{-1} to the broad peak near 3,400 cm^{-1} (assigned to Si–OH vibration) was found to increase from a to f, indicating Si–CH=CH_2 groups replace the surface Si–OH groups and its number increases with increasing additions of VTES in the bulk xerogels. This result is full in line with the discussion of structure modification in Sect. 3.1 and is similar to that shown by Matsui et al. [30].

3.3 Emission spectra

The fluorescence emission spectra of samples *a–f* (Fig. 2) show a broad band ranging from 550 to 700 nm, attributed to the emission from the triplet MLCT excited state (^{3}MLCT) to the ground state transition [31]. It is interesting that a remarkable increase in fluorescence intensity was found with increasing additions of VTES in the bulk xerogels. As the VTES/TEOS molar ratio increases up to 4:1, the luminescence intensity of composite xerogels reaches maximum and it is enhanced by 18.2 times. Further increasing of VTES results in decrease of luminescent intensity. The proper explanations for this may be as follows.

Firstly, as described in Sect. 3.1, the surface Si–OH groups are replaced by Si–CH=CH_2 groups and its number decreases with increasing additions of VTES in the bulk xerogels, resulting in subdued quenching effect between Ru(II) complexes and Si–OH groups. Secondly, surface hydrophobicity increases as a function of VTES content in the bulk precursor xerogels, which effectively inhibit luminescence quenching by H_2O molecules [14]. But further improving hydrophobicity will not guarantee the enough solubility for indicator $[Ru(Phen)_2Dppz]^{2+}$ in ORMOSILs matrix [14] and the strong self-quenching and triplet-triplet annihilation between Ru(II) complex in composite xerogels may decrease the emission efficiency. Under our preparation conditions, the optimized molar ratio of VTES to TEOS is 4:1.

The emission maximum wavelength shows red-shift from 579 to 594 nm as increasing the molar ratio of VTES to TEOS in precursor xerogels, which is more clearly depicted in Fig. 3. By relating this fact to the structure characteristics discussed above, it can be explained by the so-called "rigidochromism" originally termed by Wrighton and Morse [32]. The rigidity of the xerogels decreases with increasing additions of VTES in precursor, which results in a red-shift in the emission.

3.4 Dependence of sensitivity on VTES percent in matrix

Sensitivity of oxygen sensing materials was defined by I_0/I_{100}, where I_0 and I_{100} denote the fluorescence intensities under 100% nitrogen and 100% oxygen condition, respectively. Figure 4 shows sensitivity dependence on the

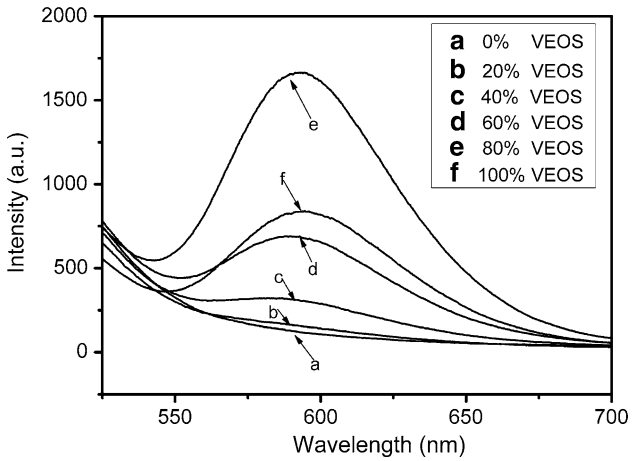

Fig. 2 Room temperature emission spectra recorded for covalently grafted VTES/TEOS composite xerogels in air. **a** 100% TEOS; **b** 80% TEOS/20% VTES; **c** 60% TEOS/40% VTES; **d** 40% TEOS/60% VTES; **e** 20% TEOS/80% VTES; **f** 100% VTES

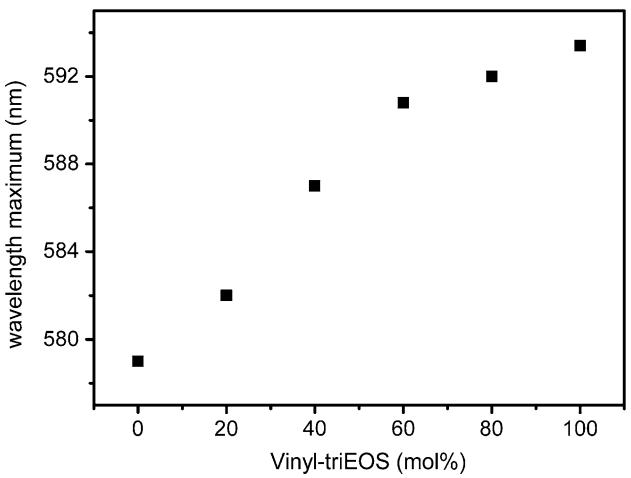

Fig. 3 Sensitivity of composite xerogels. **a** 100% TEOS; **b** 80% TEOS/20% VTES; **c** 60% TEOS/40% VTES; **d** 40% TEOS/60% VTES; **e** 20% TEOS/80% VTES; **f** 100% VTES

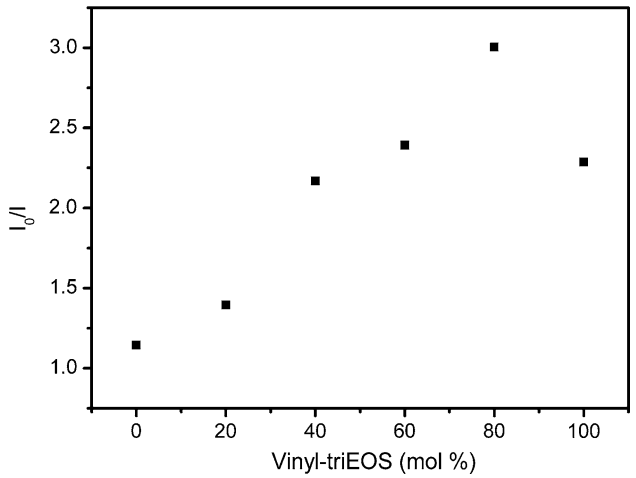

Fig. 4 Fluorescence emission peak position as a function of increasing additions of VTES

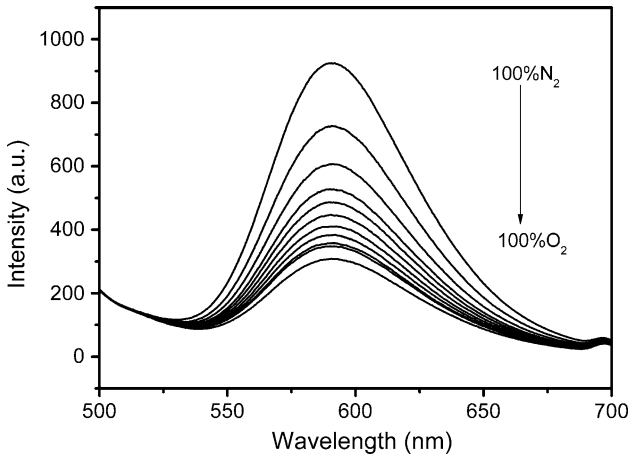

Fig. 5 Room temperature emission spectra recorded for typical covalently grafted 20% TEOS/80% VTES composite xerogels under different oxygen concentrations

molar ratio of VTES to TEOS. It is obvious that the sensitivity increases from 1.1 to 3.1 with increasing additions of VTES in precursor matrix and reaches the maximum as the molar percent of VTES is 80%. We attributed the increasing sensitivity to the enhancement of fluorescence intensity and effect of non-bridging Si–CH=CH_2 bonds, including more open structure and more hydrophobic condition, that improve oxygen permeation in media. However, as further increasing the VTES molar percent to 100% in xerogels, sensitivity decreases to 2.3, because dominant luminescent intensity greatly decreases.

3.5 Study of oxygen sensing properties

For the VTES/TEOS composite xerogels, the sensitivity was enhanced greatly and reached 3.1 by optimizing the molar ratio of VTES to TEOS. Under our preparation conditions, sample *e* (containing 80 mol% VTES in precursor) is optimal, exhibiting the maximum sensitivity. It is well known that a sensor with I_0/I_{100} more than 3.0 is a suitable oxygen sensing device [33]. Sample *e* could be used to develop oxygen sensing materials and its oxygen sensing properties are studied below.

The room temperature emission spectra, which are recorded for sample *e* under different concentrations of oxygen, are presented in Fig. 5. The position and shape at 592 nm MLCT emission from $Ru(phen)_2(Dppz\text{-}Si)Cl_2$ is constant under different oxygen concentrations. However, the relative intensity decreases markedly with increasing the oxygen concentration. The relative luminescent intensities of the $Ru(phen)_2(Dppz\text{-}Si)Cl_2$ decrease by 66.7% upon changing from pure nitrogen to pure oxygen.

Optical sensors based on the luminescence quenching are examined by the Stern–Volmer relationship. In homogeneous media with a single-exponential decay, the Stern–Volmer equation with dynamic quenching is as follows [34]:

$$I_0/I = \tau_0/\tau = 1 + K_{SV}\, pO_2 = 1 + \kappa\tau_0\, p_{O2} \quad (1)$$

which relates the ratio of the steady-state intensities or lifetime in the absence of quencher (I_0 and τ_0) to the intensity or lifetime in the presence of quencher (I and τ) through the dynamic Stern–Volmer quenching constant, K_{SV}, the bimolecular quenching rate constant that describes the collisional encounter kinetics between the luminophore and quencher, K_q, and the quencher concentration [Q]. For this ideal case, a plot of I_0/I or τ_0/τ versus [Q] (called the Stern–Volmer plot) will be linear with a slope equal to K_{SV} and an intercept of unity. The lifetime decay of luminophore in homogeneous media can be described by a single exponential equation [35]:

$$I(t) = \alpha \exp(-t/\tau) \quad (2)$$

where $I(t)$ is the luminescence intensity at time t, and α is the pre-exponential factor. However, if luminophores are immobilized in two or more sites within the silicate matrix simultaneously in which one site is more heavily quenched than the others, the Eq. 1 above is generally not obeyed and the Stern–Volmer plots become nonlinear. Several quenching mechanisms have been proposed. The simplest being the two-site familiar Demas model, which in its basic approach, assumes that the oxygen concentration is uniform but the lifetime and quenching constants are different [17], The intensity Stern–Volmer equation becomes:

$$I_0/I = 1/[f_{01}/(1 + K_{SV1}pO_2) + f_{02}/(1 + K_{SV2}pO_2)] \quad (3)$$

where f_{0i} is the steady-state fraction of light emitted from the i site and K_{svi} is its Stern–Volmer constant.

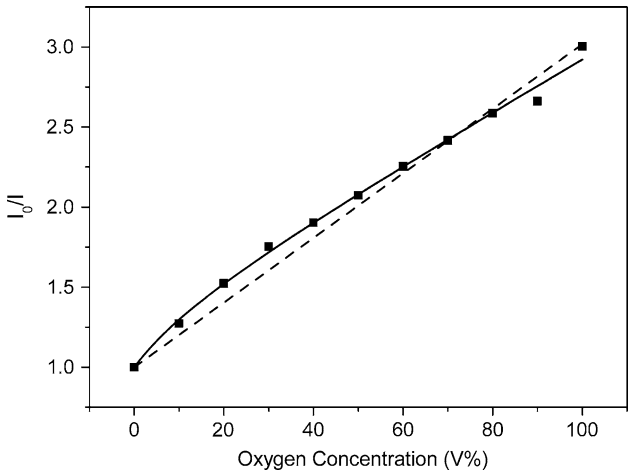

Fig. 6 Typical Stern–Volmer plot of the typical covalently grafted 20% TEOS/80% VTES composite xerogels, the scatter points in the figure is the experimental data, the solid line is the two-site Demas modelfitting result, and the dash line is the Stern–Volmer model fitting result

In Demas two-site models, there are two excited-state lifetime components for the luminescence species, and the excited lifetime decay analysis may be described by

$$I(t) = \alpha_1 \exp(-t/\tau_1) + \alpha_2 \exp(-t/\tau_2) \quad (4)$$

where $I(t)$ represents the fluorescence intensity at time t, the subscripts 1 and 2 denote the assigned lifetime components, and α_i denotes the pre-exponential factors. The weighted mean lifetime τ_m can be calculated by the following equation [17]:

$$\langle \tau_m \rangle = \sum_{i=1}^{2} \alpha_i \tau_i / \sum_{i=1}^{2} \alpha_i \quad (5)$$

Figure 6 presents the Stern–Volmer plot for sample *e*. The solid lines represent the best fits to the data. The recovered fitting parameters are compiled in Table 1. All the results show that the plot is non-linear and can not be fitted by Eq. 1 well. It has been demonstrated that non-linear Stern–Volmer plots and non-exponential excited-state decays are often obtained when quenching takes place in a solid matrix [14]. The deviation from linearity is attributed to a distribution of slightly different quenching environments for the luminophore. It is believed that there

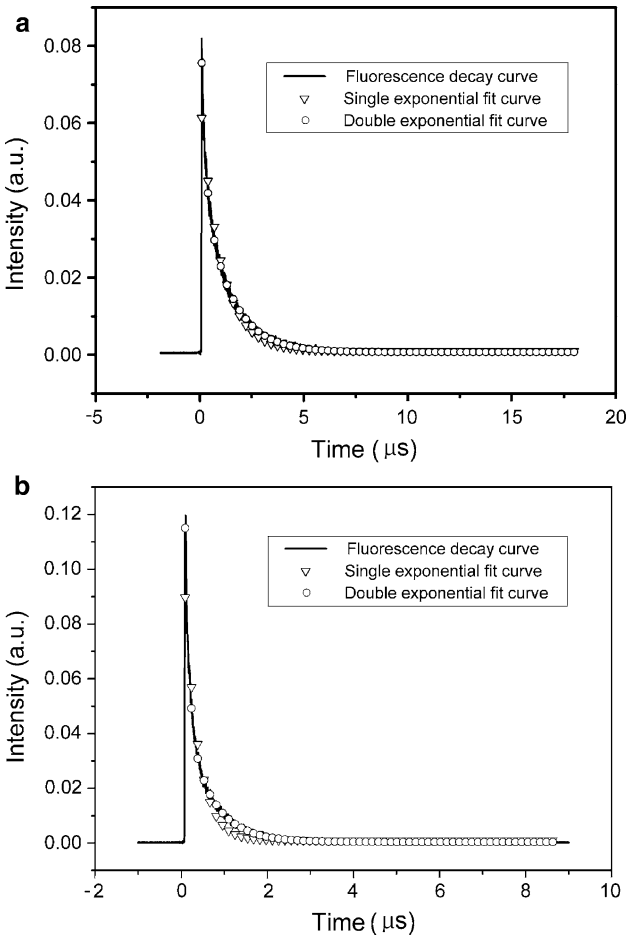

Fig. 7 Typical excited-state intensity decay profile for the covalently grafted 20% TEOS/80% VTES composite xerogels merured in the presence of pure N_2 (**a**), and in the ambient atmosphere (**b**). The scatter line is the best fit to the experimental data using the double exponential model in both (**a**) and (**b**)

are two main types of $[Ru(phen)_2Dppz]^{2+}$ micro-environments within the ORMOSIL matrix: oxygen-easy accessible and oxygen-difficult accessible sites [35]. And the Demas two-site model [6, 17] can fit the intensity-quenching curve very well.

Figure 7 shows the typical excited-state intensity decay profile for sample *e* measured in the presence of pure N_2 (a) and in the ambient atmosphere (b) along with fits to single

Table 1 Intensity-based Stern–Volmer oxygen quenching fitting parameters for 80% VTES/20% TEOS composite xerogels (sample *e*)

Samples	I_0/I_{100}	Stern–Volmer[a]		Demas[b]			
		$K_{SV}([O_2]^{-1})$	r^2	$K_{SV1}([O_2]^{-1})$	$K_{SV2}([O_2]^{-1})$	f_{01}^c	r^2
e	3.04	0.02158	0.88099	0.24885	0.00491	0.52	0.99974

[a] When an entry is not listed, the Stern–Volmer model is the best given

[b] Terms are from Eq. 3

[c] $f_{01} + f_{02} = 1$

Table 2 Time-resolved intensity decay constants for 80% VTES/20% TEOS composite xerogels (sample *e*)

Sample	Gas	α_1	τ_1(ns)	α_2	τ_2(ns)	$<\tau>$ (ns)[a]	r^2
80% VTES/20% TEOS composite xerogels(sample e)	N_2	0.05 ± 0.01	1291.4 ± 2.82	0.05 ± 0.01	187.1 ± 1.44	1143.1	0.9978
	Air	0.05 ± 0.01	597.98 ± 1.92	0.19 ± 0.01	87.34 ± 0.44	418.35	0.9971

[a] The lifetime measurements are calculated by Eq. 5

and double exponential decay models. The recovered decay terms are collected in Table 2. It is observed that the sample *e* exhibits double-exponential excited-state decay process and the decay time τ_1 and τ_2 were found to give well fit respectively. The results of the excited-state intensity decay profiles are consistent with the Stern–Volmer plot (as shown in Fig. 6). It means that the Ru(II) complex molecules are distributed simultaneously between two sites within the ORMOSILs, in which one site is more heavily quenched than the other.

It is important to determine the concentrations of molecular oxygen (O_2) in liquid phase. In order to investigate whether the luminophore leaches into the liquid phase, complex-leaching experiments were performed for the covalently-grafted incorporated sample (sample *e*) by soaking them in water, DMF and ethanol at 60 °C in a sealed cuvette under magnetic stirring and then dried at 100 °C in vacuo, as described previously [36]. This investigation reveals that the covalently-grafted composite xerogels possess greatly enhanced chemical durability. The integrated fluorescence intensities of the unquenched MLCT emission of the covalently-grafted sample after stirring in each solvent for 5 days are nearly constant and the leaching effect is small enough to be neglected. This result reveals that the Si–CH_2 covalent bonds between the Ru(II) complex and the silica matrix can effectively prevent the dopant leaching. This result is similar to that of the previously report [36].

4 Conclusion

A novel Ru(II) complex $Ru(phen)_2(Dppz\text{-}Si)Cl_2$ (phen = 1,10-phenanthroline, Dppz-Si = alkoxysilane-modified dipyrido[3,2-a:2′,3′-c]phenazine compound), containing hydrolysable silica source was synthesized and a series of composite xerogels covalently grafted with $Ru(phen)_2(Dppz\text{-}Si)Cl_2$ were prepared. The high hydrophobicity of the ORMOSILs provided by VTES, acting as an organic modifier results in enhanced luminescence and sensitivity to oxygen molecules. The luminescence intensity was enhanced by 18.2 times and the sensitivity was enhanced from 1.1 to 3.1 by optimizing the molar ratio of VTES to TEOS. These results presented here emphasized the significance of ORMOSIL as a matrix for oxygen-sensing. Their anti-leaching ability makes them promising candidates for monitoring the dissolved oxygen in liquid phase.

Acknowledgements The authors gratefully thank the financial supports of One Hundred Talents Project from Chinese Academy of Sciences and the National Natural Science Foundations of China (Grant No. 50872130).

References

1. Hitchman ML (1978) Measurement of dissolved oxygen. Wiley, New York
2. Xu H, Aylott JW, Kopelman R, Miller TJ, Philbert MA (2001) Anal Chem 73:4124. doi:10.1021/ac0102718
3. McDonagh C, MacCraith BD, McEvoy AK (1998) Anal Chem 70:45. doi:10.1021/ac970461b
4. Rosenzweig Z, Kopelman R (1995) Anal Chem 67:2650. doi:10.1021/ac00111a024
5. Bacon JR, Demas JN (1987) Anal Chem 59:2780. doi:10.1021/ac00150a012
6. Carraway ER, Demas JN, DeGraff BA, Bacon JR (1991) Anal Chem 63:337. doi:10.1021/ac00004a007
7. Li X-M, Ruan F-C, Ng W-Y, Wong K-Y (1994) Sens Actuators B 21:143. doi:10.1016/0925-4005(94)80016-2
8. Demas JN, DeGraff BA (1991) Anal Chem 63:829A. doi:10.1021/ac00017a001
9. Li X-M, Ruan F-C, Wong K-Y (1993) Analyst (Lond) 118:289. doi:10.1039/an9931800289
10. Hench LL, West JK (1990) Chem Rev 90:33. doi:10.1021/cr00099a003
11. Klein LC (ed) (1988) Sol-Gel technology for thin films, fibers, preforms electronics and specialty shapes. Noyes, Park Ridge, NJ
12. McEvoy AK, McDonagh CM, MacCraith BD (1996) Analyst (Lond) 121:785. doi:10.1039/an9962100785
13. Murtagh MT, Shahriari MR, Krihak M (1998) Chem Mater 10:3862. doi:10.1021/cm9802806
14. Chen X, Zhong Z, Lia Z, Jiang Y, Wang X, Wong K (2002) Sens Actuators B Chem 87:233. doi:10.1016/S0925-4005(02)00241-1
15. Malins C, Fanni S, Glever HG, Vos JG, MacCraith BD (1999) Anal Commun 36:3. doi:10.1039/a808731h
16. Zhang H, Li B, Lei B, Li W, Lu S (2007) Sens Actuators B Chem 123:508. doi:10.1016/j.snb.2006.09.036
17. Lei B, Li B, Zhang H, Lu S, Zheng Z, Li W, Wang Y (2006) Adv Funct Mater 16:1883. doi:10.1002/adfm.200500737
18. Sprintschnik G, Sprintschnik HW, Kirsch PP, Whitten DG (1977) J Am Chem Soc 99:4947. doi:10.1021/ja00457a010
19. Che G, Su Z, Li W, Chu B, Li M (2006) Appl Phys Lett 89:103511. doi:10.1063/1.2345826
20. Li HR, Lin J, Zhang HJ, Li HC, Fu LS, Meng QG (2001) Chem Commun Camb 13:1212. doi:10.1039/b102160p

21. Li H, Yu J, Liu F, Zhang H, Fu L, Meng Q, Peng C, Lin J (2004) N J Chem 28:1137. doi:10.1039/b401673d
22. Ossipov D, Zamaratski E, Chattopadhyaya J (1999) Chim Acta 82:2186. doi:10.1002/(SICI)1522-2675(19991215)82:12<2186::AID-HLCA2186>3.0.CO;2-1
23. Bukowski RM, Ciriminna R, Pagliaro M, Bright FV (2005) Anal Chem 77:2670. doi:10.1021/ac048199b
24. Tang Y, Tehan EC, Tao Z, Bright FV (2003) Anal Chem 75:2407. doi:10.1021/ac030087h
25. McDonagh C, Bowe P, Mongey K, MacCraith BD (2002) J Non-Cryst Solids 306:138. doi:10.1016/S0022-3093(02)01154-7
26. Li X, King TA (1996) J Non-Cryst Solids 204:235. doi:10.1016/S0022-3093(96)00420-6
27. DeWitte BM, Commers D, Uytterhoeven JB (1996) J Non-Cryst Solids 202:35. doi:10.1016/0022-3093(96)00171-8
28. Kamiya K, Yoko T, Tanaka K, Takeuchi M (1990) J Non-Cryst Solids 121:182. doi:10.1016/0022-3093(90)90128-9
29. Peng C, Zhang H, Yu J, Meng Q, Fu L, Li H, Sun L, Guo X (2005) J Phys Chem B 109:15278. doi:10.1021/jp051984n
30. Matsui K, Tominaga M, Arai Y, Satoh H, Kyoto M (1994) J Non-Cryst Solids 169:295. doi:10.1016/0022-3093(94)90325-5
31. Ding JJ, Li B, Zhang HR, Lei BF, Li WL (2007) Mater Lett 61:3374. doi:10.1016/j.matlet.2006.11.106
32. Wrighton M, Morse DL (1974) J Am Chem Soc 96:998. doi:10.1021/ja00811a008
33. Huo C, Zhang H, Zhang H, Zhang H, Yang B, Zhang P, Wang Y (2006) Inorg Chem 45:4735. doi:10.1021/ic060354c
34. Stern VO, Volmer M (1919) Phys Zeitschr 20:183
35. Han BH, Manners I, Winnik MA (2005) Chem Mater 17:3160. doi:10.1021/cm047770k
36. Li HR, Lin J, Zhang HJ, Fu LS, Meng QG, Wang SB (2002) Chem Mater 14:3651. doi:10.1021/cm0116830